Received: 2 January 2024 | Revised: 11 June 2024 | Accepted: 13 June 2024

DOI: 10.1002/gea.22016

RESEARCH ARTICLE

Geoarchaeology An International Journal WILEY

Operation and decline of the Barbegal mill complex, the largest industrial complex of antiquity

Cees W. Passchier[1] | Gül Sürmelihindi[1] | Pierre-Louis Viollet[2] | Philippe Leveau[3] | Christoph Spötl[4]

[1]Department of Earth Sciences, Johannes Gutenberg University, Mainz, Germany

[2]Société Hydrotechnique de France, Paris, France

[3]Aix Marseille Université, CNRS, CCJ, UMR 7299, Aix-en-Provence, France

[4]Institute of Geology, University of Innsbruck, Innsbruck, Austria

Correspondence
Cees W. Passchier, Department of Earth Sciences, Johannes Gutenberg University, 55128 Mainz, Germany.
Email: cpasschi@uni-mainz.de

Scientific editing by Kevin Walsh.

Funding information
Deutsche Forschungsgemeinschaft; H2020 Marie Sklodowska-Curie Actions

Abstract

The Roman mill complex of Barbegal in France is the largest preindustrial structure in Europe. Carbonate incrustations that formed from water flowing through basins, over flumes and waterwheels of the mill complex are partly preserved. The largest carbonate fragments are derived from three wooden flumes that once served the wheels of three mills in a train of eight. The deposits formed from the same water as it moved down from mill to mill. The shape, microstratigraphy and stable isotope patterns of the deposits of each flume reveal a unique history of use for each mill during the last 8 years of operation until their final abandonment. The sidewall carbonate deposits of the flumes vary in shape due to differences in the slope of the flumes during operation, associated with different-size millwheels in different basins. At least one of the flumes must have been mobile and was uplifted to fit a millwheel of a different size. During 8 years, two millwheels were exchanged and one flume was taken out of action. Carbonate deposits from two flumes were subsequently reused for some unknown industrial purpose in a water basin, and one was later embedded as spolia in a building during late antiquity.

KEYWORDS
aqueduct carbonate, archaeology, hydraulics, Roman technology, watermill

1 | INTRODUCTION

Nearly a century ago, in 1937–1939, Fernand Benoit excavated a complex ruin near the Barbegal Estate in southern France and proved that it was a unique complex of flour mills, driven by an aqueduct (Benoit, 1940). During the excavation in 1938, he found fragments of carbonate with imprints of wood, which Benoit rightly identified as having formed as a carbonate crust on the decayed wooden elements of the mills. The fragments are now in the Musée Départemental Arles Antique and were first described in Sürmelihindi et al. (2018). These deposits represent only a fraction of the original carbonate crusts that covered the woodwork of the mills, but enough material remains to shed light on the structure of the mill machinery and its operation. This is a unique opportunity since it is hard to obtain information on the structure and operation of the mills from the architectural remains. Carbonate deposits in ancient water systems can provide information on the number of years a water structure operated, the flow conditions and the environment in which it formed, for example, an open or closed channel (Sürmelihindi & Passchier, 2023). From the deposits, it is possible to reconstruct how some of the mills of Barbegal were operated and maintained, and how they were modified and finally deserted. It is important to have such information, since there are indications that the mill complex was used for some other purpose than milling grain in late antiquity (Leveau, 1995; Leveau et al., 2000, 2019). Indications on the gradual decay or sudden

abandonment of a water system can provide important insight into local societal organization and on economic and political climate that cannot be obtained in any other way. This paper provides new information on the final operation of the Barbegal mills and serves to emphasize the feasibility and power of carbonate deposits as a versatile archive to study ancient water systems.

2 | STUDY SITE

One of the first industrial-scale complexes in European history, the water mill complex of Barbegal in southern France provides unique insight into the achievements of hydraulic engineering in Roman times (Figure 1). The mill complex was built in the second century C.E. (Benoit, 1940; Leveau, 2006; Wilson, 1999) as a modification to the water supply system of the Roman city of *Arelate*, present-day Arles, France. The original first-century C.E. city aqueduct channel had two feeding branches, from the north and south sides of the Alpilles hills, which met in a convergence basin just north of the future site of the Barbegal mills (Figure 1a,b). From this basin, a single aqueduct bridge carried the joined waters across a shallow valley, the 'Vallon des Arches', to a limestone ridge south of the main Alpilles range, and then continued to the city of Arles (Figure 1b-aqw). In the second century C.E., the northern aqueduct branch was extended to the northeast side of the Alpilles range to capture additional springs, while the entire southern branch was detached at the site of the basin and used to feed the newly conceived Barbegal mill complex by a new eastern parallel aqueduct bridge across the Vallon des Arches (Figure 1b-aqe: Leveau, 1995; Leveau et al., 2000; Sürmelihindi et al., 2020). The Barbegal complex consisted of 16 water wheels in two rows of eight in a symmetric fashion, with buildings

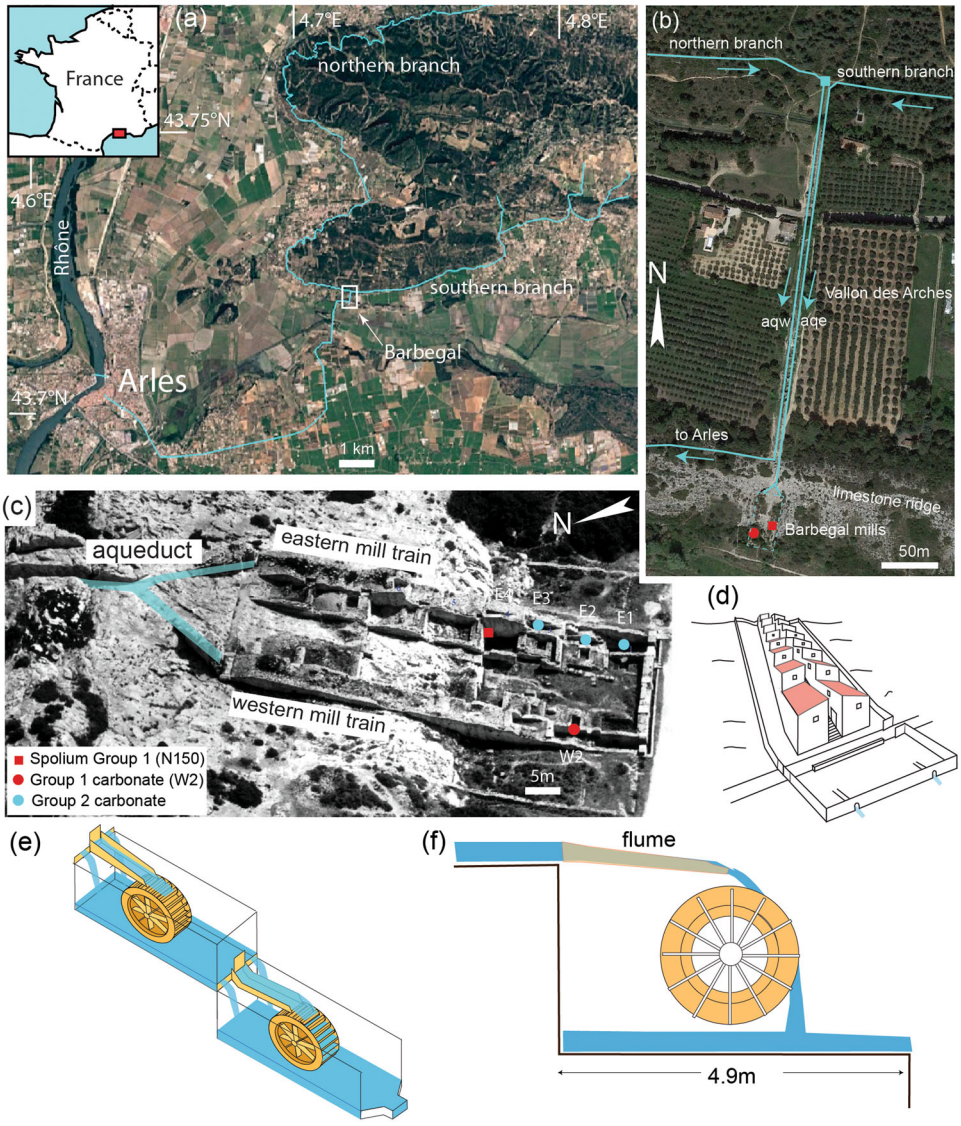

FIGURE 1 Setting of the Barbegal mill complex and in situ carbonate deposits. (a) Position of the aqueduct of Arles and the Barbegal Mills in France. Only part of the northern branch is shown. (b) Aerial view of the Vallon des Arches, with arrangement of the city aqueduct of Arles (aqw), and the aqueduct feeding the Barbegal mills (aqe). (c) Aerial view of the Barbegal mills, looking east. Red (Group 1) and blue (Group 2) markers in (b, c) indicate where carbonate fragments or in situ deposits occur on site. (d) Reconstruction of the mill complex. (e) Schematic presentation of two superposed mill basins with flumes as discussed in this paper. (f) Cross section through a mill basin with millwheel and flume.

housing the mill machinery on the inside of the mill basin trains, and an access corridor in the centre (Figure 1c,d; Sürmelihindi et al., 2020).

Carbonate deposits accumulated during the mill's operation until they ceased functioning in the third century C.E. (Leveau, 1995, 2006; Leveau et al., 2000, 2019). During excavation of the Barbegal mill complex in 1937–1939, many loose fragments of carbonate were discovered that had formed on the wooden gutters (flumes) and waterwheels of the mills (Figures 2–5; Benoit, 1940; Leveau et al., 2019; Passchier et al., 2020; Sürmelihindi et al., 2018, 2019). Carbonate was found (1) in situ in the preserved parts of aqueduct channels and mill basins; (2) as loose fragments in the debris that covered the architectural remains of the mills; and (3) as building material from late antiquity in the walls of the aqueducts and mill buildings (Figure 1, Leveau et al., 2019; Passchier et al., 2020; Sürmelihindi et al., 2018, 2019, 2020). In this paper, we present new observations made on the largest fragments of carbonate casts found in the ruins of the mill complex, originally deposited on wooden flumes that fed the wheels of the mills. A carbonate cast of an elbow-shaped flume was interpreted by Passchier et al. (2020). Recently, we identified several large carbonate fragments that could be re-assembled into two long slabs that originally formed on the bottom and walls of two other flumes of the mills with the same stratigraphy as the elbow-shaped one, but with an unusual distribution of the carbonate stratigraphy. This motivated us to attempt a reconstruction of the use of these flumes and to compare them with the flume that we described in Passchier et al. (2020). Together, the three flumes provide a tentative insight into the last stages of activity of the mill train where these flumes were used.

3 | MATERIALS AND METHODS

3.1 | Macroscopic characterization—The mills and provenance of the fragments

Each mill train consisted of eight mills in sequence on the slope of the hill (Figure 1c–e). The mill basins or wheel pits are 1.1 m wide and 4.9 m long (Figure 1f). The upper mill basins are 2.4 m deep and the two lowest ones are 2.6 m deep. Only three basins are partially preserved on the west side of the mills. None of these basins contains carbonate deposits, except for minor carbonate deposits formed by splashing water, left in the axle window of basin W2 (Figure 1c). This suggests that these basins were cleaned of carbonate deposits at some stage. Unfortunately, only limited information is preserved on the provenance of the carbonate samples of the mills during the excavations of 1937–1939 by Fernand Benoit. Fernand Benoit's archives, kept in Avignon at the Palais du Roure, contain handwritten notes providing some details on the discoveries made during the Barbegal excavations in 1938. It is noted that in June of that year, he carried out the 'removal of the limestone deposits of waterfall no. 1 on the right'. In the note, he suggested that they had formed on 'waterwheel paddles' (N138?) and on a wooden channel. He observed that 'the great canal' was 'standing leaning on the back wall (north) as if it had slipped'. On the following July 25–29, the excavation of basin 2 above basin 1, one where the wheel fragment was located, led to the discovery of two further large carbonate fragments broken into several pieces. Unfortunately, reading difficulties and the allusive nature of these notes hamper

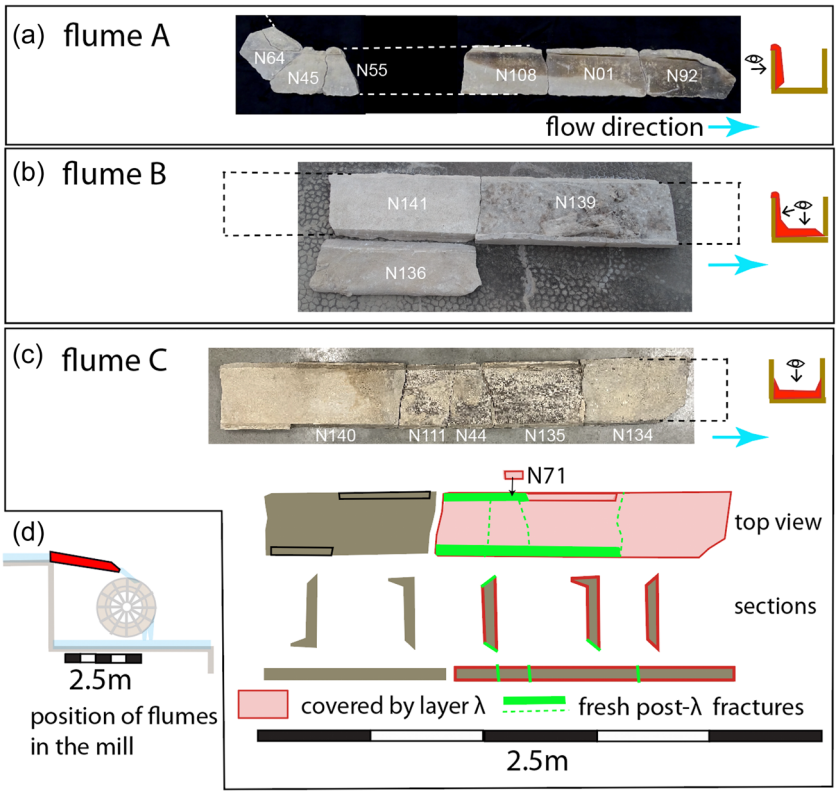

FIGURE 2 Carbonate deposit fragments re-assembled into elongate slabs that once covered the sidewall or bottom of three flumes from the Barbegal mills. Insets on the right show the position of the remaining deposits in the flumes and view direction. (a) Sidewall deposits of flume A. These have an elbow shape and were extensively analysed in Passchier et al. (2020). (b) Bottom and sidewall deposits of flume B with debris captured in the last layers of the deposit. (c) Bottom and sidewall deposits of flume C. The right-hand part of the fragment assemblage (except for N140) was later reused in a water basin and covered all around with a thin layer (λ) of new deposits, shown in red in the reconstruction sketch and sections. Green lines and markings indicate sites of fractures postdating the deposition of this layer λ. Blue arrows indicate the inferred flow direction. (d) Setting of the flumes in the Barbegal watermills.

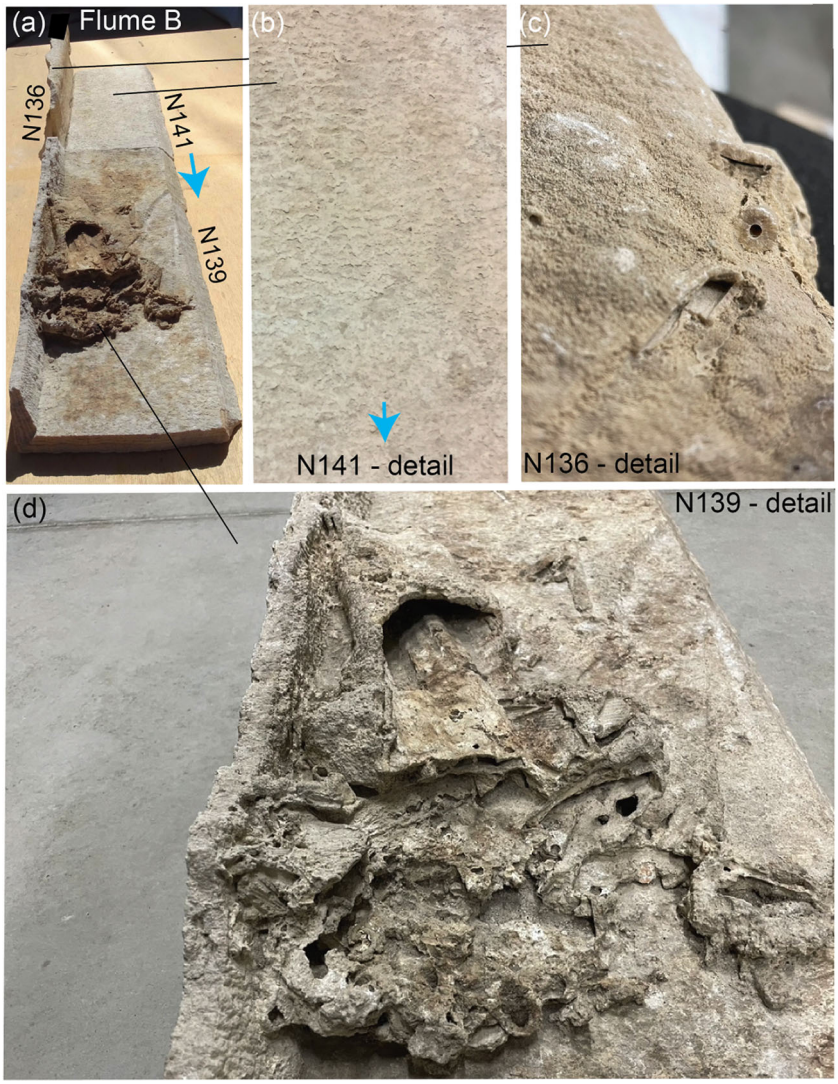

FIGURE 3 Details of the carbonate fragments of flume B. (a) Frontal view of flume B fragments showing wood debris imprints in carbonate. (b) Ripple-like structures indicating flow direction towards the front (blue arrow). (c) Detail of plant and wood debris impressions on the top of the sidewall deposits. (d) Detail of the debris imprints. Width of fragments N139 and N141 is 29 and 30 cm respectively.

their use.[1] No further information is available. Similar information is given in Benoit (1940).[2] The notes, therefore, seem to indicate that the fragments were found in basins E1 and E2, the lowest on the eastern side of the mill complex (Figure 1c). Since the stratigraphy of the large carbonate fragments is of Group 1, and the eastern basins contain carbonate similar to Group 2, the large fragments cannot have been in situ, but were transported there, possibly for later use in the eastern basins.

3.2 | Macroscopic characterization—The carbonate fragments

We exclusively worked on the collection in the Musée Départemental Arles Antique, where 142 carbonate fragments from Barbegal are stored, unfortunately without documentation. Proof that these fragments come from the Barbegal site is provided by the presence of small fragments of carbonate in the mortar layer that covers the eastern sidewall or the ruins at the height of the fourth mill basin from the bottom (basin E4). These fragments have the same stratigraphy as those in the museum and have recognizable wood imprints on one side. The mortar that contains the fragments is not Roman but was presumably added by the excavation team to strengthen and protect the top of the walls.

We have labelled the fragments preserved in the Arles museum (N1–N142) in an earlier study and published a catalogue in Sürmelihindi et al. (2019, their fig. B1). Millrun flumes had a mean inner width of ca. 0.3 m, determined from the width of preserved carbonate segments from flume bottoms (Figure 2).

[1]Notes on the carbonate fragments. [ ] indicates unreadable text: « Juin 1938—Recherche de la chute d'eau de droite. Enlèvement des dépôts calcaire de la chute d'eau n° 1 de droite (dépôt de palettes de roues à aubes?) Voir dimensions de la roue de Venafro. N.B. dépôts de canal de bois [ ] et palettes [ ] dépôts expriment convexité d'une planche de palette, dans le dépôt no 1. Le grand canal debout appuyé au mur de fond (Nord) comme s'il avait glissé. »

« 25 - 29 juillet: 2 grands fragments (en plusieurs morceaux) du canal supposé d'adduction d'eau du bief 2 sur le milieu supérieur de la roue à aubes de la cuve 1: incliné [ ] de l'aube 45 degrés, au niveau du ras de terre du talus interne (comme dans la cuve de droite 1, où le dépôt [du] canal était plus bas, à 1/2 du fond). »

[2]Benoit, 1940, page 49 «en outre de longues plaques d'empreintes calcaires avec retour à angle droit, formées à l'intérieur d'une canalisation de bois, ont été retrouvées, brisées en plusieurs fragments et inclinées à 45° au pied même des chutes d'eau des deux biefs inférieurs: il y a tout lieu de penser que ce sont les dépôts formés dans le buses dont la section serait alors de 0 m.35. La hauteur d'eau ne dépassant pas 0 m.25 d'après l'épaisseur du dépôt formé sur les parois latérales. »

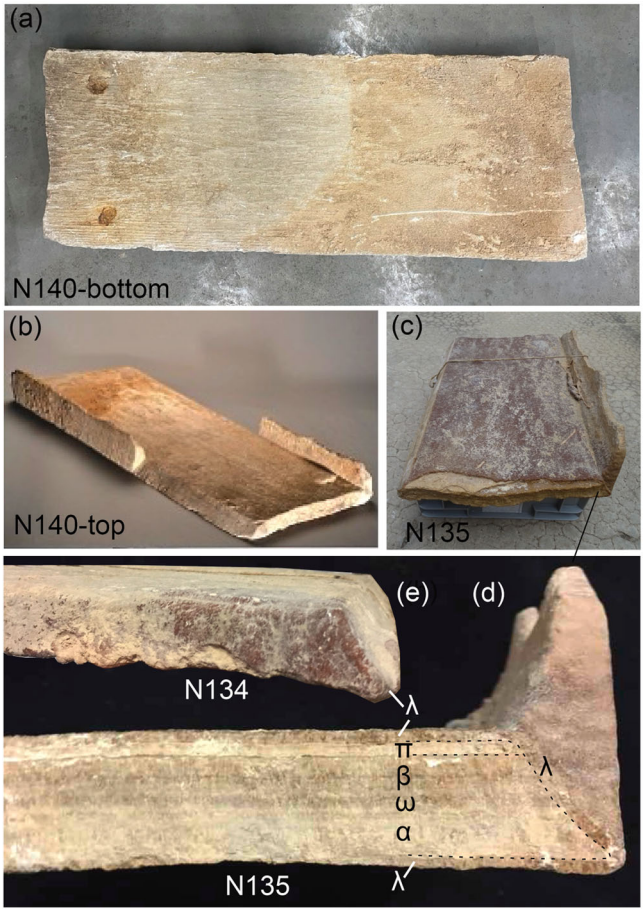

FIGURE 4 Details of carbonate fragments of flume C. (a) Bottom of fragment N140 of flume C, which lacks covering by layer λ. Impressions of the wood of the flume and of two iron nails are visible. The nails were probably used to fix the flume to the edge of the mill basin. (b) Top of N140 with low tapering sidewall deposits. (c) Fragment N135, showing low sidewall deposits on the right. The entire flume is covered by brown sparitic layer λ. This layer is broken off at the front, revealing underlying lighter-coloured primary deposits. (d) Detail of fragment N135 showing on the frontal broken surface how layer λ wraps around the older stratigraphy. λ covers an older fracture of the sidewall deposits on the right. (e) Tip of fragment N134 of flume C, wrapped with layer λ, which covers broken 45° sides where sidewall deposits were once attached (on the right) and the fracture at the front. Width of fragments N140 and N135 is 29 and 30 cm respectively.

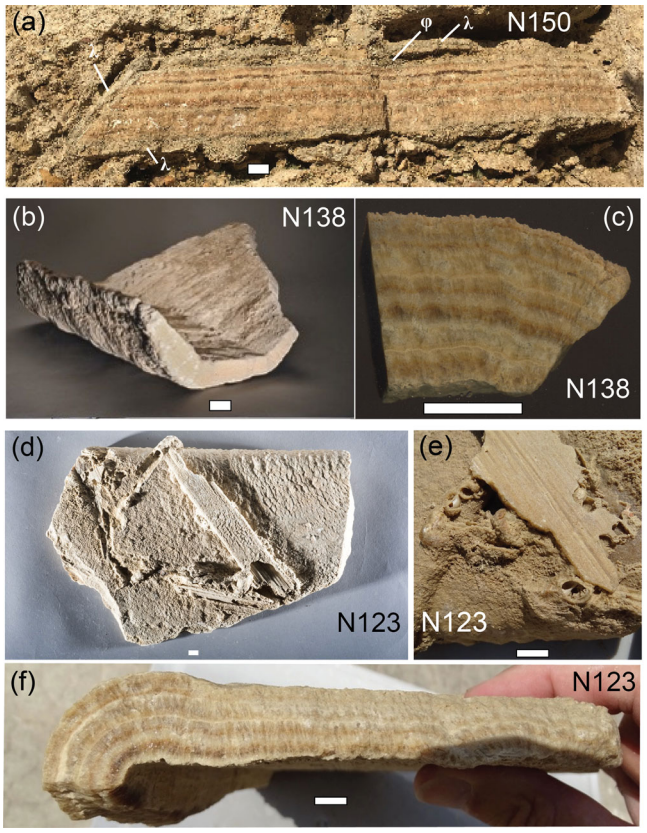

FIGURE 5 Details of smaller carbonate fragments treated in this paper. (a) Fragment N150 embedded as a spolium in the wall or a late building on the Barbegal site. This fragment once covered the bottom of a flume, has identical stratigraphy as flume A and may have been part of the bottom deposits of this flume. It was covered first by a thin layer of porous carbonate (φ) and was then wrapped all around by layer λ. (b) Carbonate cast N138, probably derived from the bottom of a millwheel bucket. (c) Stratigraphy of N138, like flume A and N150, but with the first layers missing. (d) Fragment N123, interpreted as coverage of a millwheel paddle or bucket, with shorter stratigraphy than N138. It is covered with casts of wood and other debris. (e) Detail of the impressions of debris on the surface, notably fragments of wood and *cocciopesto* and shells of freshwater snails. (f) Side view of N123. Scale bar 1 cm.

3.3 | Hydraulic modelling

Hydraulic calculations for flumes served to estimate water depth (H_f) and outflow velocity (V_f) for a given discharge. The model flume was 0.3 m wide, 0.18 m high and 2.0 m long, with an estimated roughness coefficient $Ks = 70\ m^{1/3}\ s^{-1}$ for the sides and bottom. Both elbow-shaped and straight flumes were modelled. The angle between the upper leg and the outrun leg was 40° for elbow flumes. For calculations, the flume was assumed to be unobstructed despite the observed debris in flume B (Figure 3) since this debris was only deposited in the very last stage of deposition. Due to the rectangular shape of the flume cross-section, hydraulic calculations were straightforward, based on classical equations for one-dimensional steady free surface flows (cf. Viollet et al., 1998; White, 1994). All hydraulic calculations were performed using an iterative procedure with an Excel spreadsheet. It was assumed that water was freely flowing from the upper wheel pit basin to the flume. Calculations were carried out from upstream to downstream for supercritical flow in the flume, assuming a critical section at the flume entrance. In case of a transition towards subcritical flow through a hydraulic jump, the subcritical part of the flow is calculated from the downstream condition (critical section at the exit) to the upstream, until hydraulic jump relationships are encountered. All calculations were carried out for a flume with an open end, as the final width of a possible nozzle was not preserved.

3.4 | Stable isotopes

Analyses of stable oxygen and carbon isotopes were carried out at the University of Innsbruck. Polished slabs of all samples were micromilled at 0.2 mm intervals in traces 5 mm wide and parallel to the lamination. The sample powders were analysed using a semi-automated device (Gasbench II) linked to a ThermoFisher Delta V Plus isotope ratio mass spectrometer. Isotope values, expressed as $\delta^{18}O$ and $\delta^{13}C$, are reported on the VPDB scale, and long-term precision is better than 0.1‰ for both $\delta^{18}O$ and $\delta^{13}C$.

4 | RESULTS

4.1 | Carbonate fragments

Loose carbonate fragments deposited initially on the wood of the mills can be separated into two main groups by their stratigraphy, labelled Groups 1 and 2 (Sürmelihindi et al., 2018, 2019). Group 1 deposits have very uniform stratigraphy with a regular alternation of dark and light layers representing less than 9 years of mill activity (Figures 2–5). All larger retrieved carbonate fragments and many small fragments belong to this group, partially sharing the same stratigraphy (Sürmelihindi et al., 2018, 2019). The largest Group 1 fragments are from mill flumes (Figures 2–4). Group 2 deposits are more complex (Sürmelihindi et al., 2018, 2019, 2020) and are not discussed here.

Smaller fragments of Group 1, which did not form in flumes but probably on the wood of the mill wheels (Figure 5a,b,f), commonly have incomplete stratigraphies because the wood was frequently renewed (Sürmelihindi et al., 2018, 2019). The microstratigraphy of Group 1 fragments shows a strong resemblance with deposits found in the axle window of mill basin W2 (Sürmelihindi et al., 2019), and fragments with Group 1 stratigraphy are therefore thought to have been deposited in the western mill train (Figure 1c).

4.2 | Flume fragments

Several of the larger carbonate fragments of the Barbegal mills with Group 1 stratigraphy formed on the bottom and sides of flumes and broke apart with a characteristic 45° fracture upon decomposition of the supporting wood (Sürmelihindi et al., 2019) (Figures 2c, 3a, and 4b–d; Supporting information: File S1). The carbonate mantling of three flumes, labelled A, B and C, could be partially reconstructed (Figure 2). These flume deposits differ in the details of their stratigraphy and in the geometry of the sidewall deposits. Because of their length and differences in stratigraphy, the three flumes are thought to have functioned in three separate mills on the western side of the mill complex, all part of the same mill train and operating with the same water (Figure 1e). The sequence of the three flumes in the mill train remains unknown.

4.2.1 | Flume A

The remains of carbonate that covered flume A are composed of several fragments, mainly from the sidewalls of the channel (N64, N45, N55, N108, N01 and N92) (Figure 2a) and a small fragment from the bottom (N49). Passchier et al. (2020) described these fragments in detail and can serve as a reference for the other flumes (Figure 2). The reconstructed flume had a minimum length of 1.78 m and was probably 2.1–2.2 m long (Passchier et al., 2020).

The stratigraphy of flume A consists of approximately six alternating dark and light layers (Figure 6a). The microfabric, presented in Passchier et al. (2020), is composed of thick layers of elongate columnar sparitic calcite crystals, alternating with thin layers of micrite (Supporting Information: File S2). After a sharp boundary, the dominantly sparitic main stratigraphy (layers α-ε) is covered by 5–10 mm of porous micritic carbonate (φ) with plant imprints and fragments of *cocciopesto*[3] plaster and clastic sediment, contrasting the clean, sparitic deposits of the main sequence (Figure 6a; Supporting Information: File S1). These porous deposits have mostly disappeared by erosion but are locally preserved (Passchier et al., 2020).

Maximum thickness of layers is present in the bottom fragment (N49) and the base of the sidewalls (Figure 6a). The downstream sidewall deposits of flume A have a typical hook-shaped geometry due to overflow and represent the full height of the sidewall of the flumes (Figure 6a; Passchier et al., 2020). Individual layers gradually become thinner towards the top so that overflow deposits are only slightly thinner than deposits at the base of the flume walls, while all stratigraphic layers are present at the top (Figure 6a).

4.2.2 | Flume B

Flume B consists of large fragments, two from the bottom (N139, N141) and one from sidewall deposits (N136) that combine into a coherent cast with a length of 1.56 m (Figures 2b and 3a). The stratigraphy α-ε of the bottom deposits is identical to those of flume A but is covered by a 2–3 mm wide sparite layer ζ, representing 1–1.5 years of younger carbonate deposits (Figure 6b). Unique for flume B is the preservation of carbonate casts of a mass of debris on the bottom section and some smaller casts on the sidewall deposits embedded in layer ζ (Figures 2b, 3a,c,d; Supporting Information: File S1). This debris consisted mainly of small thin pieces of worked wood, pieces of *cocciopesto*, small stones, shells of freshwater snails and roots or other plant fragments. On fragment N136, wood and plant fragment imprints are present near the top of the sidewall (Figure 3c). The covering of debris by carbonate may have taken place partly during transport in the

[3]In previous papers, we used '*Opus Signinum*' for Roman ceramic-bearing mortars, but Cifarelli et al. (2019) suggest using the Italian 'cocciopesto' instead, since *Opus Signinum* was originally used for another type of building material.

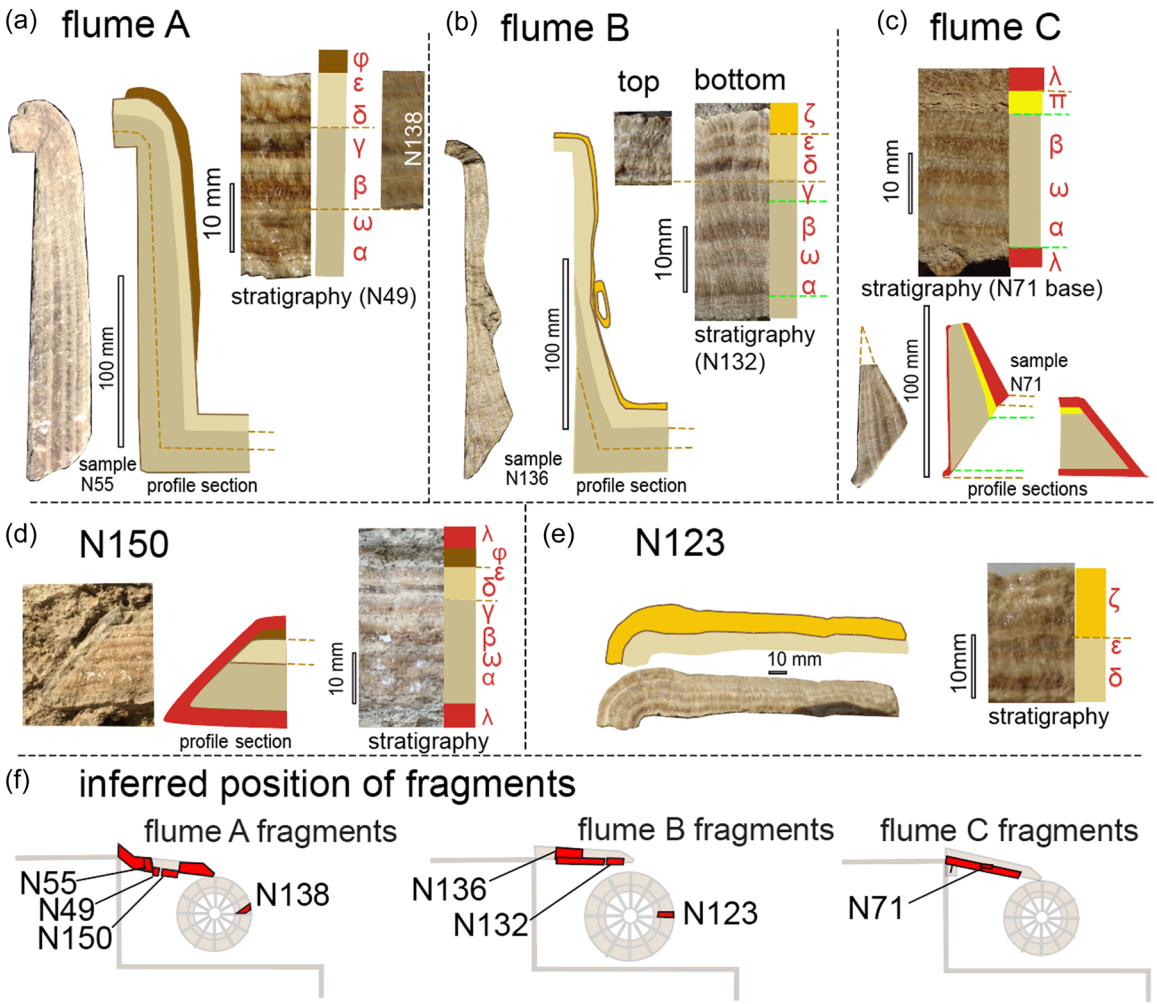

FIGURE 6 (a–c) Carbonate deposits from wooden flumes of the Barbegal mill complex. For each flume type, a cross-section through the side wall deposits, a stratigraphic profile and a schematic profile are shown. Greek letters are those used in Passchier et al. (2020) and refer to dark layers. One representative fragment (N49, N136 and N71) is shown for each flume. (d) N150 has the same main stratigraphy α-φ as flume A but is wrapped by an extra layer (λ). (e) N123 shares layers δ-ζ with flume B and is likely part of a mill bucket. (f) Inferred position of the flumes and other fragments discussed in this paper in the Barbegal mills. Labels mark fragments shown in (a–c) and in Figure 7.

channel and partly after emplacement. Small scaly ripple-like structures (Keenan-Jones et al., 2022) on top of base fragment N141 indicate that water transport was from N141 to N139 (Figure 3b).

The stratigraphic thickness distribution in sidewall deposits of flume B, preserved in plate N136 (Figure 3a, 6b), differs significantly from the sidewall deposits of flume A (Figure 6a). N136 shows an abrupt decrease in layer thickness about halfway through its height.[4] A strongly tapering base is followed by thinner upper wall deposits, while water overflowed at the top (Figure 6b). The first layers of the stratigraphy of N136 (α-γ) taper rapidly and end halfway through the height of the flume wall, while the top layers (δ-ζ) have nearly constant thickness to the top of the deposits and into the overflow deposits (Figure 6b). Although Flume B has essentially the same stratigraphy as flume A in its bottom deposits, the first part of the stratigraphy (α-γ) is missing at the top in the overflow deposits of Flume B (Figure 6a,b).

4.2.3 | Flume C

Six carbonate fragments (N140, N111, N44, N135, N134 and N71) combine into a 2.1 m long slab of bottom deposits of flume C (Figures 2c and 4). This flume has stratigraphic similarities with flumes A and B, but details differ (Figure 6). Sidewall deposits are partly preserved, still attached to the bottom deposits of flume C (Figure 4b–d). Individual layers in sidewall deposits taper more strongly upwards than in flume B (Figures 4b–d and 6c). Although the

[4]Since the large fragments of Barbegal are cultural heritage, we did not sample these deposits; photographs of the stratigraphy were made from the exposed sides, which were cleaned to see the stratigraphy. Small loose fragments with the same stratigraphy and thickness, inferred to be from the same flumes, were sampled instead for all geochemical and thin-section work.

tip of these deposits is not preserved, it seems likely that the sidewall deposits were wedge-shaped, as shown in Figure 6c, and never reached the top of the channel. The bottom deposits of flume C in segment N140 show an imprint of the wooden planks that formed the flume and of iron nails that were probably used to fix the flume to the upstream wall of the millwheel basin (Figure 4a). This implies that fragment N140 is the upstream part of the flume (Figure 2c).

The lower part of the stratigraphy has a dominantly sparitic, crystalline nature with alternating brown and transparent layers that correspond to part of the stratigraphy of flumes A and B (layers α-β: Figure 6c; Supporting information: File S2), covered by a 3–4 mm layer of micrite (layer π). An unusual aspect of flume C is that fragments N111, N44, N135 and N134 are wrapped by a 2–3 mm thick layer of sparitic, secondary carbonate (sub-stratigraphy λ). Layer λ wraps the entire deposits, top, sidewalls and bottom (Figures 2c and 4c–e). Since λ covers fracture surfaces and layers α-π of the sidewall and bottom (Figure 4d,e), the bottom plate must have broken into at least two large fragments of 1.3 m (fragments N111, N44, N135 and N134) and 0.7 m (N140) after deposition of π, and before λ was deposited on the longer fragment (Figure 2c). The longer fragment broke up further after deposition of λ. The shorter fragment of flume C (N140) was never covered by λ.

A small carbonate fragment, N71, with identical stratigraphy as flume C, including layer λ, could be sampled to make thin sections and carry out a stable isotope analysis for flume C (Figure 6c,f; Supporting Information: File S1). N71 is thought to have broken off the sidewall of N135, N44 or N111 (Figures 2c and 6c,f).

4.2.4 | Other fragments

Some other fragments with the stratigraphy of Group 1 are relevant for the reconstruction of the function of flumes A and B.

N150 (Figure 5a) is a carbonate fragment from the bottom of a flume found embedded in the wall of a building on the east side of the mill complex (Figures 1c and 5a). This fragment has the same stratigraphy (α–ε) as N49 and the flume A sidewall, including a layer of porous micrite on the top, probably φ (Figures 5a and 6d). N150 is completely wrapped by the same layer of sparitic carbonate (λ) as flume C is, including the 45° fractures where sidewall deposits were originally attached and the porous covering layer φ (Figure 5a).[5] Possibly, this fragment was part of the original bottom plate of the elbow flume A or the bottom deposits of another flume with identical stratigraphy (Figure 6f).

N138 (Figures 5b,c and 6a,f) is a fragment of unusual shape interpreted as the cast of a wheel bucket (Figures 5b,c and 6f; Passchier et al., 2020). It has the same stratigraphy as flume A but lacks layers α and ω and therefore started to form approximately 2 years after the start of the stratigraphy of flume A (Figure 6a-inset).

N123 (Figures 5d–f and 6f) is a fragment that covered the side and top of a wooden plank and has the same stratigraphy as flume B, but lacks layers α-γ (Figures 5f and 6e). Pieces of wood debris, *cocciopesto* plaster and shells of freshwater snails are attached to its top, embedded in layer ζ (Figure 5e). The minimum width of the wooden plank on which N123 formed is 185 mm (Figure 5d), more than the height of the reconstructed sidewalls of flumes A and B (175 mm; Passchier et al., 2020; Sürmelihindi et al., 2019). The deposits are thickest in the curved part of the fragment (Figure 5f). N123 is, therefore, interpreted as part of a millwheel paddle or bucket, with the curved part representing its end.

4.3 | Stable isotope patterns

Stable isotope patterns of oxygen and carbon, expressed as $\delta^{18}O$ and $\delta^{13}C$, can be used to cross-correlate stratigraphies, to establish the duration of deposition of aqueduct carbonate, and eventually to determine the duration of the mill activity (Figure 7).[6] Oxygen isotope ratios commonly show annual cyclicity due to seasonal temperature variations in the water channel (Passchier et al., 2020; Sürmelihindi, Passchier, Baykan, et al., 2013; Sürmelihindi, Passchier, Spötl, et al., 2013; Sürmelihindi & Passchier, 2023), while carbon isotope values may vary with the relative contribution of soil and bedrock components, in response to percolation speeds of water through the aquifer (Sürmelihindi & Passchier, 2023). As a result, $\delta^{18}O$ usually reaches maximum values in winter and $\delta^{13}C$ usually reaches maximum values in summer (Sürmelihindi, Passchier, Baykan, et al., 2013; Sürmelihindi, Passchier, Spötl, et al., 2013; Sürmelihindi & Passchier, 2023). The $\delta^{18}O$ and $\delta^{13}C$ patterns and microstructure of stratigraphic sections α-ε of flumes A (N49) and B (N132) (Figure 6f)[7] are mostly identical (Figure 7a,b; Supporting Information: File S2). The stable isotope patterns indicate that stratigraphy α-γ formed in 4.5 years and stratigraphy δ-ε formed in 2–2.5 years, in total representing a little more than 7 years of mill activity (Figure 7a,b). The first mill activity started in the middle of winter (year 1) and ended while approaching the summer of year 7 for the watermill hosting flume A (Figure 7a). It is possible, however, that the deposit formed over a longer time span if there were interruptions in the mill activity, for example, in year 3. In flume B, layer ζ, covering ε, represents an additional 1–1.5 years of deposition into the summer of year 8 (Figure 7b). The stable isotope profiles in both flumes A and B display a difference in mill activity between α-γ and δ-ε. There is a 'rough' high-frequency signal throughout the deposition of α-γ, which transforms abruptly into a smoother profile in δ-ε (Figure 7a,b).

The stable isotope pattern of flume C can be correlated with the top of layer α and layers ω and β of the stratigraphy of flumes A and

[5]This fragment N150 could not be sampled since it is part of a protected monument. See note 4.

[6]The stable isotope patterns were not measured on the main large carbonate fragments shown in Figure 2, but on small associated fragments that could be sampled for laboratory studies. See note 4.

[7]Fragments N49, N132 and N71 are small carbonate fragments with identical stratigraphy to the larger fragments of flume A, B and C, respectively, which have been sampled and used for laboratory analyses. See footnote 4.

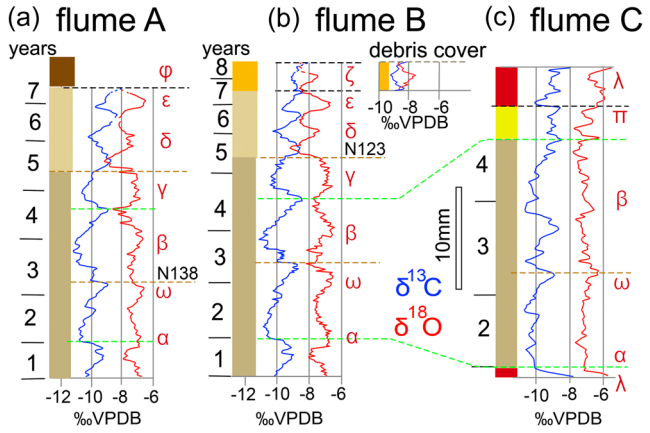

FIGURE 7 Stable isotope profiles of flumes A, B and C measured in fragments N49, N132 and N71 (Figure 6f). High values of $\delta^{18}O$ are interpreted as winter deposits and low values are interpreted as summer deposits. Profiles of flumes A and B taken from bottom deposits, and flume C from the base of the sidewall deposits. A profile from a fragment of carbonate that originally covered wood debris in flume B is shown separately. Dotted brown lines mark the start of the stratigraphy of fragments N138 and N123, interpreted as parts of millwheel deposits. Green dotted lines link shared stratigraphy of C with A and B.

B, although the pattern shows local deviations and individual layers are thicker (Figure 7). Apparently, this flume started operation 1 year after flumes A and B, probably replacing an older flume. It then operated for 2.5 years, depositing exclusively columnar sparitic carbonate without the micritic intercalations of flumes A and B (Supporting Information: File S2). This sequence is closed by a sharp break, after which carbonate is dominantly micritic and microsparitic (layer π) (Supporting Information: File S2). The flume was mantled by secondary carbonate λ, with a distinct stable isotopic profile (Figure 7c). This forms the bottom and top of the stable isotopic profile, with a pronounced final increase in stable isotope values (Figure 7c). The transition from π to λ is sharp, as can be seen in the $\delta^{13}C$ pattern, transforming abruptly into more negative values (Figure 7c).

5 | DISCUSSION

5.1 | Water level in flumes A and B

Stratigraphic comparison of carbonate deposits of flumes A and B (Figures 6a,b and 7a,b; Sürmelihindi et al., 2019) suggests that both flumes formed in the western basins of the mill complex (western mill train: Figure 1c). Since water was provided by a single aqueduct and moved down the slope from one mill basin to the next (Figure 1c,e), the deposits in both flumes must have formed from the same water in the same period of 7–8 years.

The sidewall fragments of flume A were interpreted as part of an elbow-shaped flume described by Passchier et al. (2020) (Figure 2a). The gently tapering shape of the downstream sidewall deposits of this flume proves that water was overflowing in the downstream part (Figure 6a; N55 to N92) already shortly after the flume was installed and maintained full overflowing conditions throughout the operation of the flume (Figure 6a; Passchier et al., 2020).

Flume B has a similar stratigraphy at its base as flume A, but the overflowing top of the sidewalls in fragment N136 only contains layers from the top of the stratigraphy of flume A (δ-ε), while the thickness of the sidewall deposits shows an abrupt decrease in thickness towards the top, caused by wedging out of the lower stratigraphy (α-γ) (Figure 6b). This is interpreted to be due to the low water level in flume B in the first 4.5 years of use, increasing to full capacity and continuously overflowing conditions during deposition of layers δ-ζ in the last 3 years of use (Figure 6b).

5.2 | Slope of the flumes A and B

Millwheels can be driven by flumes that deliver water on the top of the wheel (overshot) or at the side or bottom (undershot). Although Barbegal has been presented as an overshot mill by most workers (Benoit, 1940; Heimann et al., 1992; Leveau, 2006; Roos, 1986; Sagui, 1948; Sellin, 1983), some have suggested an undershot geometry (Spain, 2008, p. 15; Wefers, 2015, p. 131-132). Passchier et al. (2020) concluded that an overshot geometry is most likely in the case of elbow flume A, with a flume length of 2.1–2.2 m. For flume B, the considerable length (>1.56 m), variable water level and recorded overflow conditions also fit an overshot geometry.

The different cross-section profiles of flumes A and B must, therefore, represent a constant (overflowing) water level for flume A, and a change in water level for flume B, implying a different history of operation of the two mills served by these flumes. Flume A has partially shared stratigraphy with bucket fragment N138 (Figures 5b,c and 6a) (Passchier et al., 2020) and flume B with the proposed mill wheel fragment N123 (Figures 5d–f and 6e).

Flume A is interpreted as an elbow-shaped flume (Passchier et al., 2020), but flume B may have had a different geometry. The preserved segment of flume B has no known connection to an elbow segment and may have been part of an ordinary, straight overshot flume. The variable water level in flume B supports this interpretation, as explained below. We, therefore, present B as a straight flume in our drawings (Figures 6f and 8).

The sudden change in water level in flume B could be due to a sudden increase in discharge in the flume or a change in its slope. Flume A, which transported the same water as flume B, was permanently overflowing (Passchier et al., 2020), so the low water level in flume B could only be caused by a diversion of part of the available water away from this flume or by a steep slope (Figure 8b,d). Low water level at a gentle slope would only be possible at a discharge in the flume below 0.03 m^3/s, not enough to drive a millwheel (Figure 8c) (Passchier et al., 2020). Also, the increase in water level during deposition of layers δ-ζ cannot be due to an increase in discharge in flume B, since this would have led to an increase in deposition rate and layer

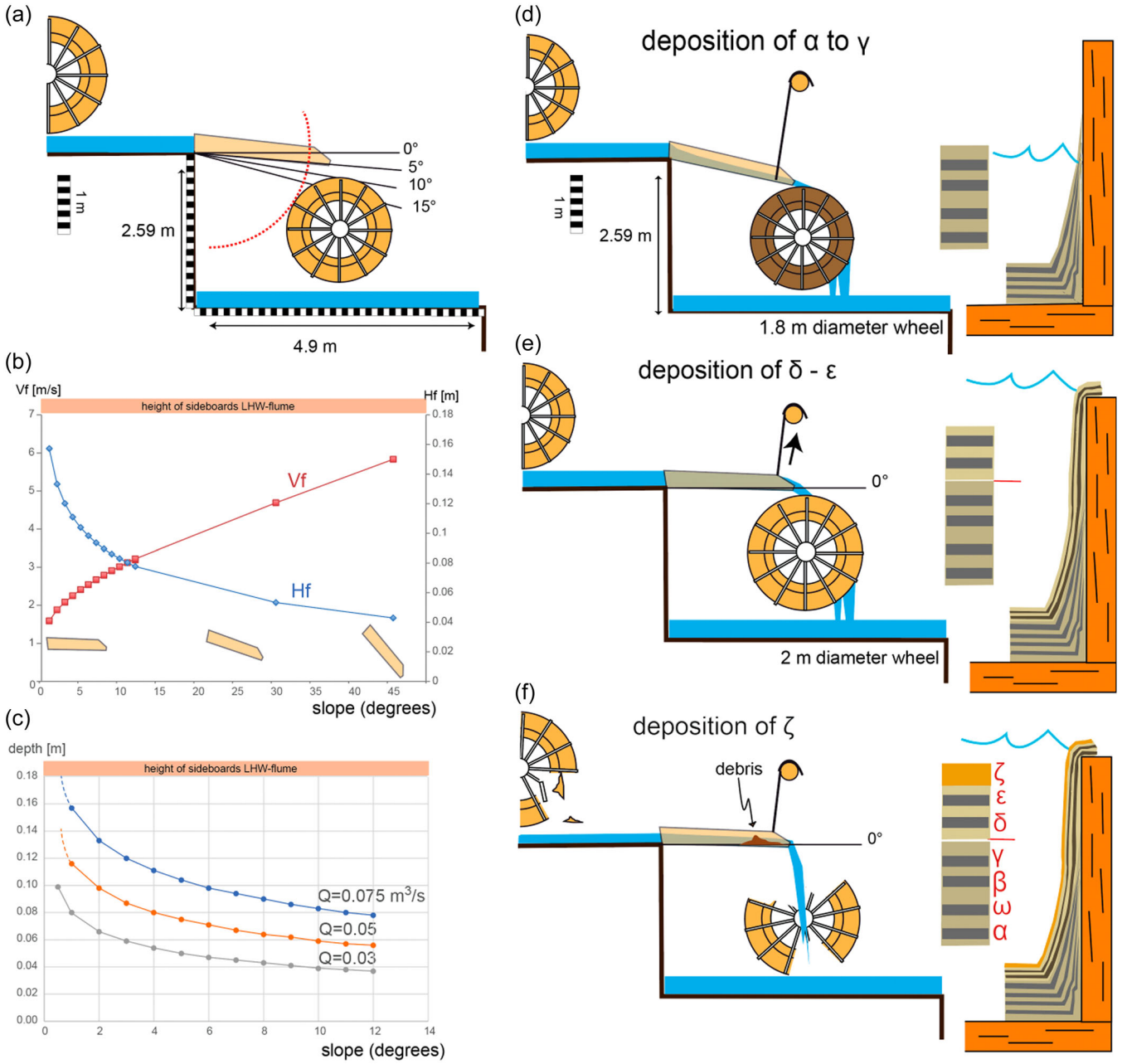

FIGURE 8 (a) Setting for flume B of the Barbegal mill, showing angles at which the flume may have been positioned. The red circle segment represents the minimum length of the flume B fragment shown in Figure 2b. (b) Water flow speeds (V_f) and water level (H_f) at the end of a 2.1 m long 0.3 m wide rectangular wooden flume for different slopes, and discharge Q_f = 0,075 m^3/s. At lower discharge, water level would be accordingly lower. (c) Water depth at the end of a straight 2.1 m long flume for different discharge values Q, within the likely range attained in the western mill train. (d–f) Reconstructed history of flume B, based on the carbonate stratigraphy. (d) After an initial steep orientation and low water depth in the flume, the flume was uplifted (e) and operated for a period in this position. In the last year of water flow (f), wood and other debris accumulated and were not removed.

thickness (Sürmelihindi, Passchier, Baykan, et al., 2013), while there is no indication for this: the thickness of the stratigraphy α-ε is about the same in the bottom section of flumes A and B (Figure 6a,b); this means that the deposition rate of carbonate was the same in flumes A and B, and that they, therefore, transported the same discharge Q_f over 7 years while layers α-ε were deposited. This discharge cannot explain overflowing in a steep flume, so the change in water level in flume B must have been due to a change of the slope of the flume to a shallower angle during deposition of layers δ-ζ (Figures 6a,b and 8). The slope of the flume was near horizontal at this time, with a V_f of 1 m/s or less, causing overflowing (Figure 8e). Flume B must, therefore, have been *mobile*, probably with a pully that could be used to change the slope (Figure 8d–e). Such mobile flumes are not uncommon in modern mills and probably in Roman mills since they allow fine-tuning

of the impact angle of water flow onto the mill wheel, depending on discharge (Müller & Kauppert, 2004; Spain, 2008, p. 78-81). Notice that a change in slope, as described here, would only work for a straight flume; the long leg of an elbow-shaped flume would not have enough space to be inclined enough to produce the observed low water levels. Interestingly, the high-frequency signal in the stable isotope patterns of flumes A and B transforms into a smoother signal after layer γ (Figure 7b), indicating some change in the depositional setting, possibly due to the change in the operation mode of the mills.

Passchier et al. (2020) estimated the mean discharge in the western mill train during the deposition of Group 1 stratigraphy, based on the discharge in flume A at 0.05–0.075 m^3/s (50–75 l/s). If flume B initially had lower H_f and higher V_f at similar Q_f as flume A, it must have been steeper. The actual slope is hard to determine, but we estimate from Figure 6b that the water level was originally 10 cm or even less. Figure 8b shows the water level in the flume for different inclination angles. The length of the flume is estimated at 2.1 m because of the dimensions of the wheel basins and the length of the water arch towards the mill wheel (Passchier et al., 2020).

Figure 8c shows the water depth at the end of a straight 2.1 m long flume for different discharge values. For a discharge of 0.05–0.075 m^3/s and water depth of 8–10 cm, the slope of a straight flume must be 4–11 degrees. At the highest discharge of 0.075 and the lowest flume water level of 8 cm, the tip of a 2.1 m long flume would be 44 cm below the bottom of the upper basin, which would leave 2.2 m for the wheel, water level in the basin and free room between both (Figure 8a): probably the angle was shallower, with a lower discharge, while the wheel was probably small, for example, 1.8 m in diameter (Figure 8d). The steep slope of the flume could have been intended to increase the kinetic energy of water hitting the wheel but would have caused considerable water spillage by splashing. The steep flume B was possibly used for a mill with other millstones than mills with shallow-dipping flumes like flume A. Alternatively, the steep slope of flume B was a first attempt to increase water flow from the basin to the flume by creating critical flow conditions at the upstream end of the flume, while later, the elbow-shaped flume A was invented to improve this effect further (Passchier et al., 2020).

5.3 | Change of millwheels

If flume B was uplifted to a permanently shallow slope after 4–5 years of operation, *why* this was done? The orientation of flumes is usually carefully regulated in overshot mills to attain the right angle of impact and water flow velocity into the buckets of the millwheel (Le Gouriérès, 2009; Passchier et al., 2020). Uplift of a flume is only needed if the position or size of the wheel is changed as well (Figure 8e). Uplift of the flume with the same wheel remaining in place would have made mill operation very inefficient due to an erroneously large distance between the flume and the wheel and an incorrect impact angle of the water into the wheel buckets (Spain, 2008, p. 78- 81). Uplifting the wheel to follow the flume tip is difficult because of the small dimensions of the axle window. A change of millwheel to a larger diameter is, therefore, the most likely adaptation.

If the geometry of carbonate deposits in flume B is due to the uplift of the flume due to a change of millwheels, it is interesting to notice that carbonate fragment N123, which is thought to be derived from a millwheel, starts at the onset of layer δ, exactly at the time when the slope of the flume is changed. Since N123 contains layers δ-ζ, including wood debris in the top layer, it could well be a carbonate fragment from the new millwheel (Figure 8f). A change of millwheel to a larger size may have been associated with a change of the type of millstones (Le Gouriérès, 2009).

According to the impressions left by wood on the carbonate of the mill flumes, the wood commonly used in the Barbegal mills was pine (Sürmelihindi et al., 2019). Such wood deteriorates in some years in the wet conditions of a mill (H. Chanson, pers. comm. 2019), and the replacement of the wheels can be seen in this light. The flumes would have to be replaced less often than wheels since they were immobile and protected by a crust of carbonate on the bottom and sides, while the wheels were strained by their motion and may have been less protected because wheel straining fractured the carbonate cover (Sürmelihindi et al., 2019).

Passchier et al. (2020) described how fragment N138 (Figure 5b,c) has identical stratigraphy as flume A, but lacks the lowest layers α and ω. This fragment was, therefore, interpreted as part of a mill wheel that replaced an older one 2 years after the start of operation of flume A, possibly also because of deterioration of the older mill wheel or a change of millstone type.

5.4 | End of flumes A and B

Deposition of sparitic carbonate in flume B continued for at least 1–1.5 years longer than that in flume A (Figures 6b, 7b and 8f). During this time, debris collected in flume B, mostly on the bottom of fragment N139, but also on fragment N136, and was covered by layer ζ (Figures 3a,c,d and 6b). The same applies to the possible wheel deposits of fragment N123 (Figures 5d,e and 6e). Fragments of worked wood and *cocciopesto* in the debris (Figure 3d) could represent material washed down from degrading mill machinery and structures upstream.

The presence of debris in flume B and on the wheel may indicate abandonment of part of the complex while the aqueduct kept running, since it is hard to conceive that such debris would be allowed to partly block the flumes of a well-maintained working mill.

In deposits of flume A, the regular sparite-dominated stratigraphy is followed by fine-crystalline and porous deposits with clastic sediments (sand grains) and imprints of plant fragments (layer φ: Sürmelihindi et al., 2019). These deposits could indicate low-flow conditions and deposition in daylight, especially if plant fragments are present (Sürmelihindi et al., 2019). This could mean that the roof structure of the mills was damaged, admitting daylight.

5.5 | Flume C

Flume C has bottom deposits with a total length of 2.1 m, suggesting that it must have been a straight flume similar to flume B, although both an overshot or undershot geometry is possible (Figures 2c and 8). The bottom deposits of flume C are of similar thickness as in flumes A and B, but with a shorter formation history of less than 3 years and greater individual layer thickness and more dominantly sparitic microfabric, suggesting a more rapid deposition rate (Figures 6 and 7; Supporting Information: File S2). Deviations in the stable isotope pattern of flume C from flumes A and B can be due to differences in operation times of the mills fed by the three flumes: individual mills could have been switched off for weeks, while others continued functioning (Sürmelihindi et al., 2019). Flume C has preserved sidewall deposits that taper sharply upwards, indicating that the water level was generally low in the flume, less than 10 cm. This observation, the fast deposition rate and the sparitic microfabric suggest that the slope of this flume was permanently steep, and steeper than flume B. However, some differences can be caused because flume C was sampled in N71, part of the sidewall deposits, and flumes A and B in the bottom deposits.[8]

Layer π, the last layer of flume C's stratigraphy, is micritic, contrasting with the earlier sparite-dominated deposits. This layer possibly formed in reaction to a sudden change in deposition conditions, which can also be seen in the stable isotope profile. Possible causes for this sudden change in fabric are low water level and slow flow, suggestive of decreased discharge and/or slower flow due to the uplift of the flume. Like layers ζ and φ, π is probably indicative of the end of the use of the mill that was fed by flume C. Flume C probably ceased operation before the uplift of flume B.

5.6 | Use of flume carbonate fragments in antiquity

Two large pieces of carbonate found in the ruins of Barbegal are mantled by a peculiar layer of secondary carbonate λ. After deposition of layer π, the bottom deposits of flume C broke into at least two large fragments, probably by decay of the wood after the mills stopped operating (Figure 2c). The longest fragment was then covered by layer λ (Figures 2c and 4c–e), while the short one (N140) escaped this fate. The same mantling happened to fragment N150 from the bottom of a flume with the same stratigraphy as flume A. This fragment was later used as *spolium* in the wall of a building from late antiquity on the east side of the Barbegal complex (Figures 1c, 5a and 6d).

Layer λ has a distinct stable isotope pattern: a sudden initial decrease in $\delta^{13}C$ values was followed by co-variation of both isotopes and ended with a sharp increase in $\delta^{13}C$ and $\delta^{18}O$ (Figure 7c). This suggests that during this last deposition, evaporation and degassing were much higher than usual, removing the lighter isotopes, and these are very likely to be in response to a change in the depositional setting (Figure 7c). Note that layer λ in flume C is not identical to layer ζ in flume B, since the microfabric and isotopic composition are different (Figure 7).

The wrapping of flume fragments by layer λ can be explained by their submergence in running water supersaturated in carbonate, like that circulating through the mills. One possibility is that this occurred when flumes collapsed into the basins while water was still running, as a final event in the history of the mills. It is curious, however, that only large flume bottom plates have been found to be covered with layer λ, and that both bottom and top and at least one side are covered, while one side is nearly bare of deposits. Fragment N71, which was part of flume C, was probably in this position: it has deposits of layer λ on its top surface, but not on the former sidewall deposits, except at the corner (Figure 6c). This implies that plates have been standing free in the water, most likely on their side. It is therefore more likely that the flume plates were used in some of the mill basins of Barbegal to compartmentalize them lengthwise. Use of the large carbonate flume bottom fragments in the mill basins also explains why the large fragments of flume bottoms were found inside the eastern basins, as described by the original excavator (Benoit, 1940), and belong to the best-preserved remains, while fragments of Group 2 are all smaller. There was no place for mill wheels in this case, so these must have been removed when the new purpose of the mill basins was set up. What this new purpose was is still unknown, but the dark colour of layer λ suggests some industrial use such as the retting of flax, the washing of wool or soaking of skins for a tannery: the area just south of Barbegal had a significant sheep farming industry in late antiquity (Badan et al., 1995).

5.7 | Reconstruction of events

Figure 9 summarizes the reconstructed history of the mills based on the observations discussed above. The relative location of the mills that hosted flumes A, B and C in the western millrun is unknown, but they must have been in sequence above each other. Timing of events in flumes A and B could be reconstructed from the $\delta^{18}O$ profile, which shows clear annual cyclicity, with winter and summer peaks (Figure 7a,b).

Flumes A and B started to operate in winter, and identical stratigraphy formed on these flumes until the summer of year 7 (Figures 6 and 7). Flume B was initially steeply inclined, possibly feeding a smaller diameter mill wheel (Figures 8d and 9), while flume A was shallow-dipping and overflowing, with a larger mill wheel. Possibly, both mills used different mill stones. In the summer of year 3, the millwheel associated with flume A was changed, possibly because of damage, and replaced with a new wheel on which fragment N138 formed (Figures 6a and 7a). It is not unlikely that the weight of accumulated carbonate contributed to this damage (Sürmelihindi et al., 2019). In the spring of year 5, flume B was uplifted to a shallow angle, raising the water level till the flume was overflowing, after which layers δ-ε formed (Figures 8e and 9). At the same time, the associated millwheel was probably changed to one with a larger diameter. Fragment N123 may have been deposited on this new millwheel. It is not clear why the size of the mill wheel was changed, but possible reasons could be adaptations to

[8]No bottom deposits of flume C could be sampled for stable isotope analysis. See footnote 4.

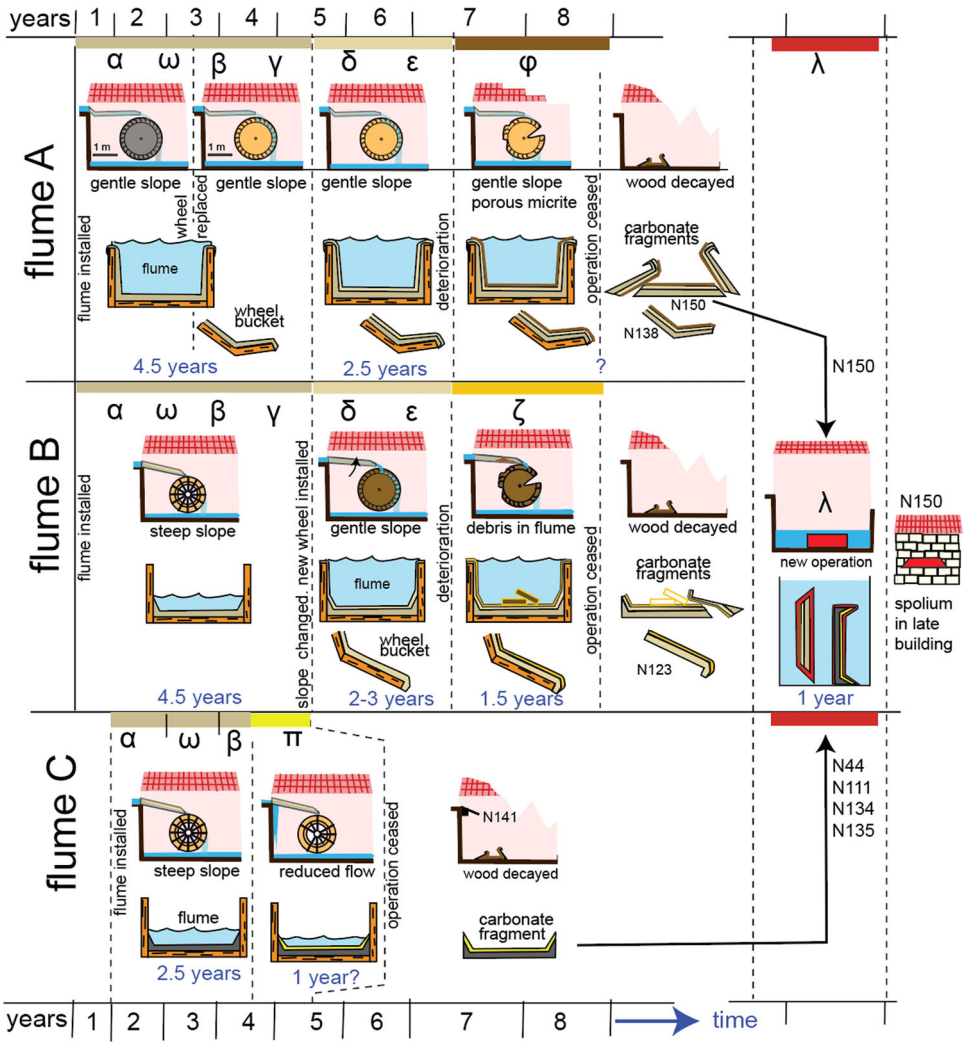

FIGURE 9 Reconstructed history for flumes A, B and C and fragments N150, N138 and N123. Each stage provides the reconstructed orientation of the flume above its mill basin, and an enlarged cross-section through the flume. Time is horizontal, and for some parts of the history, the approximate number of years for each stage can be given. The sequence of basins of flumes A, B and C in the mills is presently unknown. Two groups of fragments, from flumes A and C, were submerged at some unknown later stage in a covered basin, probably for some new purpose of the mill basins, and acquired an extra sparite layer λ. Subsequently, one of these fragments (N150) was reused as a spolium in a late-Roman building on the Barbegal site. Coloured bars indicate the position of stratigraphic segments as presented in Figure 6 and 7.

different millstone requirements, an adaptation to increase the efficiency of the mill (Passchier et al., 2020) or simply replacing with what was available. Operation then continued for approximately 2 years, till the summer of year 7 (Figures 7 and 9). Regular, sparitic deposition on flume A then halted, and porous carbonate with plant imprints and fragments of *cocciopesto* and clastic sediment was deposited (layer φ). This suggests the end of regular mill operation in the mill of flume A. In flume B and on the associated wheel, represented by fragment N123, wood debris, *cocciopesto* and plant debris accumulated over 1–1.5 years (layer ζ) until the fall of year 8, also suggesting a stop to normal mill operations, although deposition conditions were different from those in flume A: flume B probably continued to operate in the dark, inside an intact building, while flume A was exposed to daylight in a building with a ruined or dismantled roof, causing more porous deposits (Passchier et al., 2020; Sürmelihindi & Passchier, 2023; Sürmelihindi et al., 2019).

The timing of deposition in flume C is less clear than that of flumes A and B, but it may have started operation 1 year after these flumes, maintaining a steep orientation over the next 3–4 years and operating in a dark environment, producing mostly sparitic carbonate (Figure 9: Passchier et al., 2020; Sürmelihindi & Passchier, 2023; Sürmelihindi et al., 2019). The flume may have been overshot, as shown, or undershot. Finally, sparitic deposition was abruptly changed to micrite deposition (layer π), possibly due to a sudden drop in discharge over some time, signalling the end of the operation of flume C. It is presently unclear what the age of layer π is with respect to the stratigraphy of flumes A and B (Figure 9). With deposition of layers φ, ζ and π, mill activity on the western side of the Barbegal complex ceased.

At a later stage, large fragments of bottom deposits from flumes A and C were placed into basins. They were covered by sparitic carbonate (layer λ) all around, including on fractures, indicating that

the wood of the flumes had decayed and the carbonate that covered the flumes had broken into large fragments (Figure 9). A 1.3 m long fragment of flume C was entirely covered by λ. The shorter 0.7 m long fragment of flume C (N140) escaped deposition of λ, possibly because it was the uppermost part of the flume and was still on remains of wood attached to the top of a basin (Figure 9). Judging by the shape of the $\delta^{18}O$ profile and the carbonate thickness, deposition of layer λ may have lasted approximately 1 year. The sparitic, dense nature of carbonate λ suggests that deposition took place in a dark building with an intact roof (Passchier et al., 2020; Sürmelihindi et al., 2019).

Fragment N150, covered with layer λ, was later used to restore a late-Roman building of the eastern part of the complex, suggesting that the eastern part of the mill continued to operate for some purpose, even after the activity that produced layer λ (Figure 9).

The different history of flumes A, B and C, which are all derived from the western side of the Barbegal mill complex in three of its eight basins, suggests that different mills were used in different ways during the last years of operation of the mill complex.

6 | CONCLUSIONS

Carbonate fragments from flumes of the west side of the Barbegal mill complex allow detailed reconstruction of mill operation there in its final stages and provide insight into the way operation was maintained and gradually ceased.

- Mills on the west side of the Barbegal complex were used in different operational modes during the last 8–9 years of activity.
- At least some mills were overshot.
- Different mill basins may have had different types of flumes, with elbow shapes or straight.
- Some flumes were mobile and could be uplifted to deliver water to the mill wheel at the correct impact angle.
- Flume B was uplifted during its active life from a steep to a shallower angle, possibly because of the replacement of its mill wheel by one with a larger diameter.
- Abandonment of the western mills took place while the aqueduct was still running, but gradual deterioration can be observed in the changing carbonate microfabric.
- The end of the operation came in different stages for different mills of the western mill train.
- Carbonate fragments of flume A end with porous deposits, which are interpreted to represent the removal or collapse of roof structures while water flow had not yet stopped.
- The presence of wood fragments and other debris in flume B, covered with carbonate deposits, indicates the last year of operation of the western mills.
- Some carbonate from flumes was reused and placed in a roofed basin with running water for some new industrial purpose.
- Carbonate deposits can be a powerful agent that can reconstruct the operation of ancient water systems.

AUTHOR CONTRIBUTIONS

Cees W. Passchier, Gül Sürmelihindi and Philippe Leveau designed the study. Cees W. Passchier, Gül Sürmelihindi and Pierre-Louis Viollet performed the research. Cees W. Passchier and Gül Sürmelihindi sampled and analysed carbonate fragments. Cees W. Passchier and Gül Sürmelihindi analysed the data. Cees W. Passchier wrote the first draft of the manuscript. Pierre-Louis Viollet performed flume hydraulic calculations. Philippe Leveau performed the field work and archaeological analysis of the mills. Christoph Spötl provided stable isotope data. All authors read and approved the final version.

ACKNOWLEDGEMENTS

We thank Alain Charron, Conservateur en chef du patrimoine, responsible for the collections of the Musée Départemental Arles Antique and Valérie Clénas, for help during study of the fragments in the museum and for permission to sample some of the smaller fragments for further analysis. Funding by the EU scheme of Marie Curie Individual Fellowship AQUEA (890454) (Gül Sürmelihindi) and DFG projects PA578/17 (Cees W. Passchier) and SU864/2-1 (Gül Sürmelihindi) is gratefully acknowledged. Open Access funding enabled and organized by Projekt DEAL.

CONFLICT OF INTEREST STATEMENT

The authors declare no conflict of interest.

DATA AVAILABILITY STATEMENT

The data that support the findings of this study are available from the corresponding author upon reasonable request.

ORCID

Cees W. Passchier http://orcid.org/0000-0002-3685-7255
Gül Sürmelihindi http://orcid.org/0000-0001-7874-8631
Christoph Spötl http://orcid.org/0000-0001-7167-4940

REFERENCES

Badan, O., Congés, G., & Brun, J.-P. (1995). Les bergeries romaines de la Crau d'Arles. Les origines de la transhumance en Provence. *Gallia*, *52*, 263–310.

Benoit, F. (1940). L'usine de meunerie hydraulique de Barbegal (Arles). *Revue Archéologique*, *15*, 19–80.

Cifarelli, F. M., Smith, C., Colaiacomo, F., Kay, S. J., Ceccarelli, L., & Panzieri, C. (2019). Elaborazioni tecniche dell'opera cementizia nel "Lazio del Calcare" nella tarda età repubblicana: L'opus signinum e Segni. In I. Fumadó Ortega & S. Bouffier (Eds.), *Mortiers et hydraulique en Méditerranée antique* (pp. 145–166). Presses Universitaires de Provence.

Le Gouriérès, D. (2009). Les petites centrales hydroélectriques: Conception et calcul. Editions du Moulin Cadiou.

Heimann, S., Drewes, U., & Leveau, P. (1992). Abflussberechnungen für den Aquädukt von Arles und den Aquädukt der Mühlen von Barbegal. *Mitteilungen aus dem Leichtweiss-Institut für Wasserbau der Technischen Universität Braunschweig*, *117*, 534–546.

Keenan-Jones, D., Motta, D., Garcia, M. H., Sivaguru, M., Perillo, M., Shosted, R. K., & Fouke, B. W. (2022). Travertine crystal growth ripples record the hydraulic history of ancient Rome's Anio Novus aqueduct. *Scientific Reports*, *12*, 1239.

Leveau, P. (1995). Les moulins de Barbegal, les ponts-acqueducs du vallon des Arcs et l'histoire naturelle de la vallée des Baux (bilan de six ans de

fouilles programmées). *Comptes-rendus des séances de l année—Académie des inscriptions et belles-lettres*, *139*, 115–144.

Leveau, P. (2006). Les moulins de Barbegal (1986–2006). www.traianvs.net/pdfs/2006_barbegal.pdf

Leveau, P., Passchier, C., & Sürmelihindi, G. (2019). Les Moulins de Barbegal, 80 ans après les fouilles de F. Benoit. L'apport de la géoarchéologie des carbonates. In D. Djaoui & M. Heijmans (Eds.), *Arelate Intra et extra muros, Archéologie et histoire en territoire Arlésien* (pp. 111–139). Editions Mergoil.

Leveau, P., Walsh, K., Bertucchi, G., Bruneton, H., Bost, J.-P., & Tremmel, B. (2000). Le troisième siècle dans la vallée des Baux: Les fouilles de la partie basse et de l'émissaire oriental des moulins de Barbegal. *Revue Archéologique de Narbonnaise*, *33*(2000), 387–439.

Müller, G., & Kauppert, K. (2004). Performance characteristics of water wheels. *Journal of Hydraulic Research*, *42*, 451–460.

Passchier, C. W., Bourgeois, M., Viollet, P.-L., Sürmelihindi, G., Bernard, V., Leveau, P., & Spötl, C. (2020). Reconstructing the hydraulics of the world's first industrial complex, the second century CE Barbegal watermills, France. *Scientific Reports*, *10*, 17917.

Roos, P. (1986). For the fiftieth anniversary of the excavation of the water-mill at Barbegal: A correction of a long-lived mistake. *Revue Archéologique (Paris)*, *2*, 327–333.

Sagui, C. L. (1948). La meunerie de Barbegal (France) et les roues hydrauliques chez les anciens et au moyen âge. *Isis*, *38*, 225–231.

Sellin, R. H. J. (1983). The large Roman water mill at Barbegal (France). *History of Technology*, *8*, 91–109.

Spain, R. (2008). The power and performance of Roman water-mills. Hydromechanical analysis of vertical-wheeled water-mills. *BAR International Series*, *1786*.

Sürmelihindi, G., Leveau, P., Spötl, C., Bernard, V., & Passchier, C. W. (2018). The second century CE Roman watermills of Barbegal: Unraveling the enigma of one of the oldest industrial complexes. *Science Advances*, *4*(9), eaar3620.

Sürmelihindi, G., Passchier, C., & Leveau, P. (2020). Giving voice to the incrustations from a Roman watermill complex at Barbegal: An impression. In S. Bouffier, I. Fumadó Ortega, L'eau dans tous ses états. *Perceptions Antiques. Archéologies Méditerranéennes*, *1*, 161–171.

Sürmelihindi, G., & Passchier, C. W. (2023). Writ in water—unwritten histories obtained from carbonate deposits in ancient water systems. *Geoarchaeology*. *39*, 63–88.

Sürmelihindi, G., Passchier, C. W., Baykan, O. N., Spötl, C., & Kessener, P. (2013). Environmental and depositional controls on laminated freshwater carbonates: An example from the Roman aqueduct of Patara, Turkey. *Palaeogeography, Palaeoclimatology, Palaeoecology*, *386*, 321–335.

Sürmelihindi, G., Passchier, C. W., Leveau, P., Spötl, C., Bourgeois, M., & Bernard, V. (2019). Barbegal: Carbonate imprints give a voice to the first industrial complex of Europe. *Journal of Archaeological Research: Reports*, *24*, 1041–1058.

Sürmelihindi, G., Passchier, C. W., Spötl, C., Kessener, P., Bestmann, M., Jacob, D. E., & Baykan, O. N. (2013a). Laminated carbonate deposits in Roman aqueducts. *Sedimentology*, *60*, 961–982.

Viollet, P. L., Chabard, J. P., Esposito, P., & Laurence, D. (1998). *Mécanique des fluides appliquée, Presses des Ponts et Chaussées*. Cambridge University Press.

Wefers, S. (2015). Die Mühlenkaskade von Ephesos. Studien zur Technikgeschichte und zur Versorgung einer spätantiken bis frühbyzantinischen Stadt. *Monographien des RGZM*, *118*.

White, F. M. (1994). *Fluid mechanics*. McGraw-Hill.

Wilson, A. (1999). Deliveries extra urbem: Aqueducts and the countryside. *Journal of Roman Archaeology*, *12*, 314–331.

SUPPORTING INFORMATION

Additional supporting information can be found online in the Supporting Information section at the end of this article.

How to cite this article: Passchier, C. W., Sürmelihindi, G., Viollet, P.-L., Leveau, P., & Spötl, C. (2024). Operation and decline of the Barbegal mill complex, the largest industrial complex of antiquity. *Geoarchaeology*, *39*, 594–608. https://doi.org/10.1002/gea.22016